IFIP Networking 2019 1570511400

# BeamSniff: Enabling Seamless Communication under Mobility and Blockage in 60 GHz Networks

Tianbo Gu, Zhicheng Yang, Debraj Basu, Prasant Mohapatra
Department of Computer Science, University of California Davis, USA
Emails: {tbgu, zcyang, dbasu, pmohapatra}@ucdavis.edu

***Abstract*—Recently, millimeter-wave (mmWave) is augmenting popularity in wireless communications since it provides multi-Gbps throughput by exploiting the broad unlicensed 60 GHz spectrum. Highly directional adaptive beamforming antennas are inherently employed in 60GHz to counteract the severe propagation and penetration losses experienced in this spectrum. Compared to traditional omnidirectional antennas, beamforming introduces critical challenges in medium access control, especially in link establishment and maintenance. In particular, node mobility and object blockage become crucial, which necessitates frequent beam steering to re-establish links. The state-of-the-art protocols fail to jointly address both the mobility and blockage challenges. Their approaches trigger exhaustive beam search to pair antenna sectors on every link failure which produces an excessive delay that conceivably disrupts communication and lowers the quality-of-service(QoS).**

**In this paper, we propose *BeamSniff*, a novel protocol that resolves the mobility and blockage issues jointly while sustaining a seamless communication. Upon link failure, it intelligently estimates the possible cause of link failure and instantly foresees plausible paths to recover the broken link, thereby eliminating the frequent exhaustive beam search which results in reducing the overhead for link maintenance. *BeamSniff* is assessed extensively in our custom-built 60GHz system platform with a ray-tracing based simulator under various indoor environments. The evaluation manifests the efficiency of the protocol in sustaining seamless communication along with multi-fold throughput gain compared to state-of-the-art protocols. We observe up to 14× throughput increase in typical scenarios involving motion and blockage.**

***Index Terms*—60 GHz Networks, Millimeter-wave, Wireless communication, IEEE 802.11ad, Beamforming, Protocol design, Mobility and blockage**

## I. Introduction

The advancement in mobile devices technologies coupled with the mobile application industry thrusts the demand for high-speed transmission with an exponential increase. The bottleneck is still the last mile wireless link which is constrained by its spectrum shortage. 60 GHz mmWave communication is going to play an indispensable role in the next-generation wireless world due to its extraordinary data rate (up to 6.7 Gbps). However, some communication features introduced by 60 GHz are impeding its large-scale deployment. First, highly directional antennas adopted in 60 GHz require the transmission beams of the communication entities to be perfectly aligned. Second, due to weak diffraction ability, 60 GHz communication requires to transmit in non-line-of-sight (NLOS) links as the signal cannot penetrate most obstacles, such as human body.

The IEEE 802.11ad defines the beamforming training (BFT) [1] procedures for 60 GHz WLANs to find the optimal communication path with the strongest signal. The separated sub-phases sector-level sweep (SLS) and beam refinement phase (BRP) in BFT require exhaustive beam pairs scanning for link establishment. Due to the exhaustive search in the BFT, the beam training time complexity grows quadratically with the number of antenna beam sectors. Narrowing the beam width raises the number of beam sectors. The BFT overhead in 802.11ad with $22.5^\circ$ beam width is $\sim 28ms$ while the value rises to $\sim 1s$ when the beam width is reduced to $5.6^\circ$ [2]. As a link encounters mobility and blockage problems, it triggers BFT to search a new optimal path which costs lengthy link outages. The frequent link outages dismantle the QoS for common 60 GHz based applications such as virtual reality.

Existing research works combat mobility and blockage challenges *separately*. Furthermore, some works require the *additional hardware* components to assist the communication. [3] adjusts the beam direction based on the prediction of node mobility through measurements using client's accelerometer and magnetometer. Additional WiFi devices are employed in [4], [5] to assist the beam steering via inferring the client's motion direction. But these techniques require additional detection band antennas and could just detect unobstructed direct path condition. MOCA [6] is another alternative approach which selects a path through a beam-sounding mechanism every time before transmitting a data frame. These mobility related solutions fail to resolve the link failures when a fast moving obstacle continuously shadows a client. On the other hand, approaches targeting to solve the blockage problem such as BeamSpy [7], consider only stationary nodes, where human bodies or other objects may intermittently block the LOS. They restore the link quickly by utilizing the pre-searched NLOS path. But their performance in fast mobile scenarios is unacceptable. Currently, there is no immaculate protocol proposed in 60 GHz communication to deal with both the mobility and blockage problems simultaneously. Most of the proposed techniques only focus on solving either mobility or blockage issue independently.

In this paper, we investigate how a client can preserve communication in the case of device motion and human or object blockages. Then, we propose *BeamSniff*, a model-driven framework to efficiently overcome 60 GHz link vulnerability against mobility and blockage with infinitesimal cost. Upon predicting a link failure, *BeamSniff* promptly explores the best available LOS or NLOS path utilizing the real-time spatial and temporal correlations of the link state in different directions. *BeamSniff* exceedingly eliminates the frequent exhaustive beam-search which results in an exceptional boost in QoS.

ISBN 978-3-903176-16-4 © 2019 IFIP

In summary, our contribution breaks down into the following aspects:

- A novel protocol *BeamSniff* is proposed to solve mobility and blockage challenges in 60 GHz networks *jointly*. By analyzing the dynamical ambient environment, *BeamSniff* intelligently sniffs the new beam direction within the greatly compressed beam search space, thereby circumventing frequent exhaustive BFT searches.
- *BeamSniff* does not require any *additional hardware components* to assist the new communication link searching. It actively tracks and maintains a minimum portion of channel state in temporal and spatial dimensions. By exploring the correlation with past link states, *BeamSniff* determines when and how to send minimum sniffing frames and instantaneously explore a possible LOS/NLOS path in a real-time manner.
- We build a customized end-to-end 60 GHz communication system platform to conduct numerous well-designed experiments. The typical indoor mobile scenarios are analyzed involving node mobility and blockages. The unique temporal and spatial correlation of received signal strength (RSS) variation due to mobility and obstacle are investigated thoroughly.
- The performance of *BeamSniff* is evaluated in our 60 GHz system platform that shows up to *14× throughput gain* in indoor wireless communication involving mobility and obstacles. Furthermore, we build a ray-tracing based simulator for extensive evaluation of the proposed technique. The experiments validate that *BeamSniff* can maintain links seamlessly while minimizing the overheads.

## II. Background and Motivation

### A. Mobility and blockage in 60 GHz

Due to the unique directional requirement, 60 GHz channels are susceptible to node movements and LOS blockage. In this paper, device motion denotes that an STA (client) moves in free space without any obstacle in the LOS. When a device moves, the misalignment of a previously established beam pair leads to severe signal attenuation. Furthermore, 60 GHz links usually cannot penetrate the human body, mental, water, wall and other similar objects [8]. A blockage can lower the RSS up to a level that cannot even support lowest modulation and code rate for control PHY [1]. It can significantly impact the link, which is also a primary hurdle that makes 60 GHz system arduous to be broadly deployed now.

In this paper, we independently discuss the cases of device motion and blockage due to their distinct handle way for link failure. For device motion, the AP has to cooperate with the client to obtain a new LOS transmission path. While for humans and other objects related blockages, one new NLOS path requires to be sought for recovering the link.

### B. IEEE 802.11ad BFT

IEEE 802.11ad defines BFT training procedures with two sub-phase: sector level sweep (SLS) and beam refinement phase (BRP). As shown in Figure 1, in SLS phase, devices with coarse-grained sectors with quasi-omni beam pattern are

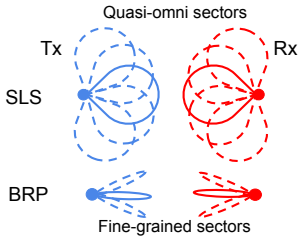


Fig. 1: BFT training in IEEE 802.11ad

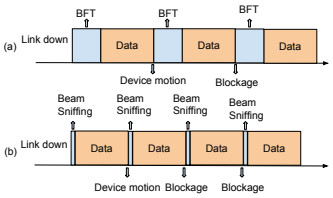


Fig. 2: IEEE 802.11ad BFT compares with BeamSniff.

paired. Subsequently, in BRP, the link is fine-tuned and an optimal link is picked. The time complexity in BFT equals $\alpha^2 + \beta^2 + c$, where $\alpha$ denotes the number of quasi-omni sectors in SLS, and $\beta$ denotes the number of fine-grained sectors with a highly directional beam in BRP. $\alpha$ is equal to $2\pi/\omega$ if both the AP and the client use the same beamwidth $\omega$. Commonly, different beamwidths are adopted considering power and functional limitations. $\beta \ll \alpha$ because the essential beam direction has already been established and only a few fine-grained beam directions are required to explore for obtaining the optimal communication link. Narrowing a beamwidth results in increasing $\alpha$ and $\beta$, which in turn increases the searching latency. The exhaustive search in the first SLS phase causes the beam training time complexity to increase quadratically $\mathcal{O}(\alpha^2)$ depending on the number of beam directions [8]. A highly directional beam can be produced employing electronic phased-array antennas. In free space, the AP and client can align their beam directions through BFT and establish the optimal communication link. However, if the client is moving or some obstacles emerge between AP and client, the link is usually broken down, and the exhaustive beam searching in BFT has to be invoked again and again. In a real indoor environment, mobility and blockage problem is inevitable, and the time costly BFT needs to be executed frequently. However, with the beamwidth of $5.6°$, the BFT overhead in 802.11ad even boosts to $\sim 1s$ [2], which is unacceptable for most real-time applications. Our approach leverages the unique spatiotemporal correlations to intelligently sniff a new link thereby bypassing frequent BFT in mobile and blockage scenarios and greatly expanding the usable time of data transmission, which is shown in Figure 2.

## III. BeamSniff Protocol Design

In this section, we illustrate the key protocol and algorithms to surmount the mobility and blockage hurdles jointly. In the rest of the paper, if there is no specific claim, we always consider the 60GHz communication in indoor environments. For outdoor situations, it is impracticable to find reflecting medium to construct NLOS paths in case an obstacle blocks the LOS link. The link fails and cannot recover due to unavailability of a signal reflector.

### A. Design overview

First, we introduce the major components used in *BeamSniff*. Then, we give the brief overview of our protocol. The detailed *MAC layer* interaction protocol will be illustrated in the following section.

***Codebook generation***: *BeamSniff* needs to rapidly alter the beam direction and also adjust the beam widths based protocol requirement. *Hierarchical codebook* [9] is adopted in our design, which exploits sub-array and deactivation (turning-off) antenna processing technique. In a 2-D antenna array, sub-array and deactivation technique can select any subsets of the array to generate different beam widths and gains in specific directions. The hierarchical codebook is layered where each layer represents a different beam width and a higher layer indicates a narrower beam. In each layer, different codewords (antenna weight vector) represent a specific beam direction with the beam width in the corresponding layer. All the codewords residing in the same layer have the same beam widths but different steering angles. We use $\mathbf{w}(k,i)$ to denote antenna weight vector of $i^{th}$ codeword in the $k^{th}$ layer corresponding to beam direction $\Omega$ and beam width $\omega$. We separate N-antennas array into M sub-array with $N_S$ antennas in each sub-array, which means $N$ equals to $M \times N_S$. Let $A(\mathbf{w}(k,i),\Omega)$ denote the beam gain of codeword **w** along with angle $\Omega$, which is defined as:

$$A(\mathbf{w}(k,i),\Omega) = \sqrt{N}a(N,\Omega)^H\mathbf{w} = \sum_{n=1}^{N}[\mathbf{w}]_n e^{-j\pi(n-1)\Omega} = \sum_{m=1}^{M}\sum_{n=1}^{N_S} e^{-j\pi(m-1)N_S\Omega}[\mathbf{f}_m]_n e^{-j\pi(n-1)\Omega} \quad (1)$$

where $\mathbf{f}_m$ can be seen as the sub-codeword of the $m^{th}$ sub-array. For specific beam width $\omega$ ($k^{th}$ layer) and beam direction $\Omega$, our goal is to select antenna weight vector $\mathbf{w}(k,i)$ to maximize $|A(\mathbf{w}(k,i),\Omega)|$ so as to get maximal gain in that beam width and direction configuration. The maximum $|A(\mathbf{w}(k,i),\Omega)|$ with beam widths $\frac{2N_A}{N_S} = \frac{2MN_A}{N}$ can be reached if we set:

$$\mathbf{f}_m = \begin{cases} e^{-jm\frac{N_S-1}{N_S}\pi}a(N_S,-1+\frac{2m-1}{N_S}) & m = 1,2,...,N_A \\ \mathbf{0}_{N_S\times 1} & m = N_A+1,...,M \end{cases} \quad (2)$$

where $N_A$ is the number of active sub-arrays. The final optimization result is based on jointly using the sub-array and deactivation method.

The codebook is generated and stored like a hashtable way. We can retrieve the system setting for the required beam angle and beam width from the pre-defined codebook in a much faster way.

***BeamSniff lookup table (BLT):*** *BeamSniff* maintains a temporal and spatial based lookup table. The table records the LOS and NLOS channel information at previous location $L_{T_l}$. Actually, *BeamSniff* only relies on the information of last time point. The lookup table is sorted by the RSS of transmission links. As shown in Table I, $AS_i^{LS}(L_{T_l},\omega_{k_0})$ denotes the $i^{th}$ beam sector with beam width $\omega_{k_0}$, which is used to construct the LOS transmission path in location $L_{T_l}$ at time $T_l$. $\omega_{k_0}$ corresponds to the beam width in $k_0$-level of the hierarchical codebook, and $i^{th}$ beam sector index denotes the beam direction with angle $\Omega = i \times 2\pi/Q_{\omega_{k_0}}$, where $Q_{\omega_{k_0}}$ represents the number of beam sectors with beam width $\omega_{k_0}$. Then the $(i-1)^{th}$ and $(i+1)^{th}$ are the adjacent beam sectors of $i^{th}$ beam sector. Meanwhile, $CS_j^{LS}(L_{T_l},\omega_{m_0})$ is used to denote the beam sector index of LOS path on the client side. The beam width $\omega_{m_0}$ could be different from AP's. Therefore, AP and client beam sector pair $[AS_i^{LS}(L_{T_l},\omega_{k_0}), CS_j^{LS}(L_{T_l},\omega_{m_0})]$ is selected to build the real LOS transmission link at time $T_l$.

TABLE I: *BeamSniff* Lookup Table

| Transmission path | AP Beam Sector | Client Beam Sector |
|---|---|---|
| LOS Link: | $AS_i^{LS}(L_{T_l},\omega_{k_0})$ | $CS_j^{LS}(L_{T_l},\omega_{m_0})$ |
| $1^{th}$ NLOS Link: | $AS_{p1,i}^{NLS}(L_{T_l},\omega_{k_1})$ | $CS_{p1,j}^{NLS}(L_{T_l},\omega_{m_1})$ |
| $2^{nd}$ NLOS Link: | $AS_{p2,i}^{NLS}(L_{T_l},\omega_{k_2})$ | $CS_{p2,j}^{NLS}(L_{T_l},\omega_{m_2})$ |
| ... | ... | ... |

In 60 GHz indoor communication, there exists only one LOS path while there may be multiple NLOS paths available. $[AS_{p1,i}^{NLS}(L_{T_l},\omega_{k_1}), CS_{p1,j}^{NLS}(L_{T_l},\omega_{m_1})]$ is an example of beam sector pair used for NLOS path, which is also shown in Table I. The RSS of NLOS paths should be above the reception cutoff, $-68$ dBm to obtain a basic data transmission rate of 385 Mbps at MCS-1. BeamSniff sorts the NLOS paths based on RSS. Although reflected paths have relatively weaker RSS than LOS path, they should be monitored and utilized when LOS link is broken down.

***Initialize and update BLT***: In the initial phase of *BeamSniff*, the AP and the client try to discover each other and establish a communication link via revised BFT procedures. In IEEE 802.11ad standard, the outcome of BFT procedures is the optimal communication link with strongest RSS. We modify the traditional BFT to generate the *BeamSniff* lookup table. An exhaustive search is executed in SLS phase to find the strongest beam sector pair from total $\frac{2\pi}{\omega_{k_0}} \times \frac{2\pi}{\omega_{m_0}}$ beam pairs, which is usually a LOS path denoted by $[AS_i^{LS}(L_{T_l},\omega_{k_0}), CS_j^{LS}(L_{T_l},\omega_{m_0})]$ with coarse-grained beam direction. But beyond that, other beam sector pairs could also be used to transmit data as backup paths if their receive sensitivity is not less than -68 dBm. Thus it records these beam sectors pairs as NLOS paths in the *BeamSniff* lookup table. *BLT* usually does not need to store the fine-grained beam sectors information obtained from the second BRP phase in BFT under high mobility and blockage scenario. Fine-grained beam sector searching is time-consuming and may lead to longer delay if communication link frequently meets outage. After initializing the *BLT*, the AP and the client cooperate with each other to continuously maintain and update the table. When and how to update the *BLT* is described in the following section.

***Link failure prediction and recovery:*** An established link is always preserved if there is no device movement or blockage. Device motion results in the sector misalignment, and obstacle blockage breaks the link. Upon frequently encountering device motion and obstacle blockage, for the IEEE 802.11ad, the exhaustive search in BFT is invoked over and over again to seek the optimal link. The performance of data transmission is severely constrained by the exhaustive search. BeamSniff intelligently sniffs the available links with much less time cost thereby extensively expanding the usable time of data transmission.

BeamSniff records the channel information in recent time

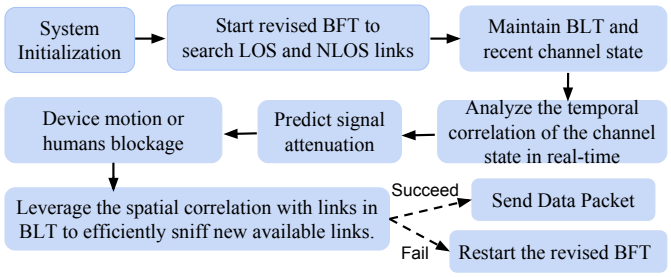


Fig. 3: *BeamSniff*'s Flow Diagram.

and leverages the historical and real-time channel information to predict the potential forthcoming link outage. In the meantime, it probes the reason for signal attenuation and takes particular actions. By leveraging spatial and temporal channel correlation from BLT, BeamSniff acquires a communication path from potential paths. In free space with device motion, current broken LOS path will be restored with new LOS path. In the case where obstacle causes link outage, a new NLOS path is procured for link recovery. The novel sniffing protocol is presented in the following section.

### *B. Beam Sniffing Protocol*

*BeamSniff* monitors the signal attenuation and foretells the link outage in real-time. Once upcoming link outage is foretold, BeamSniff starts to send sniffing frames in potential paths to explore a new LOS or NLOS transmission link. The *sniffing frame* is like the control frame in 802.11ad and consists of three parts: preamble, header, and a payload. The header carries modulation and coding scheme (MCS), length of data or a checksum. The sniffing frame can be transmitted using MCS-0 (lowest possible MCS) which provides the minimum data rate of 27.5 Mbps. Now we explain our wisely sniffing mechanism step by step as showing the flow diagram in Figure 3.

***1. Link outage prediction and reason estimation***: The first phase of *BeamSniff* is to foresee an imminent link failure. We have discerned that before a link fails, there is usually sufficient signal fluctuation to recognize it. With predicting a possible upcoming link failure, our algorithm also distinguishes the cause of link failure. Based on device motion or blockage, *BeamSniff* starts to sniff new feasible LOS or NLOS transmission paths. BeamSniff monitors the recent RSS values $[RSS(t_{i-K+1}), ..., RSS(t_i)]$ in window $K$. If the variation of current RSS value exceeds a threshold $(\Upsilon)$ compared with historical values sequence, a signal attenuation is recognized.

Although human blockage and device motion both lead to the signal attenuation, they pose distinctive attenuation patterns that we can employ to differentiate them. The RSS goes down smoothly for device motion while large attenuation fluctuation in RSS indicates a human blockage as shown in Figure 6. Link failure due to device motion or human blockage can be identified by second order statistics of RSS and handled separately. if the second order statistics of RSS values are varying too much, that indicates human blockage; otherwise, it flags a motion without blockage. The complete procedure is shown in Algorithm 1.

**Algorithm 1:** Signal attenuation detection and reason estimation

```
while Read RSS value do
    Analyze recent RSS values sequence in window K
    if (1/K) Σ_{r=i-K}^{i-1} (RSS(t_i) − RSS(t_r))^2 > ϒ then
        ∂²RSS(t, K) =
          (∂²/∂²t)[RSS(t_i), ..., RSS(t_(i+K−1))]
        if Var{∂²RSS(t, K)} > Ψ then
            Detect human blockage and start to sniff
              along the NLOS paths in BLT table.
        else
            Detect device motion and start to sniff
              along LOS paths in BLT table.
    else
        Continue to read next RSS value.
```

Based on our measurements, the success rate of link failure prediction can reach to 95.26% if we set K and $\Upsilon$ to be 5 and 1.1 respectively. Due to the obvious difference of the second order statistics of RSS values, we can distinguish the device motion or human blockage with an accuracy of 100% when the value of $\Psi$ is set to 2.5, which also matches the observation in [8]. According to the reason estimation, *BeamSniff* performs a different course of action as described in subsequent sections.

***2. Prevent link outage for device motion:*** The reason we separately analyze device motion in free space is that NLOS paths are not available in this scenario. The mechanism that BeamSniff uses to search the new available link is described as following:

***2.1 Sniff with wider beam***: Assume the current primary link to be denoted by $[AS_i^{LS}(L_{T_l}, \omega_{k_0}), CS_j^{LS}(L_{T_l}, \omega_{m_0})]$, which is established in location $L_{T_l}$. Once beam sniffing is triggered, the AP goes back to lower layer $(k_0 - 1)$ in codebook and switches to the wider beam width $\omega_{k_0-1}$ while concentrating on the same direction. AP uses the new beam sector to send sniff frames to the client. If a client can receive and decode the sniff frame successfully, it sends feedback carrying the channel state information. Upon receiving the feedback, the AP coordinates with the client to further calibrate the beam directions. Ultimately AP determines the MCS level corresponding to data rate under new established link, and use the new sector pair $[AS_{i'}^{LS}(L_{T_{l+1}}, \omega_{k_0-1}), CS_{j'}^{LS}(L_{T_{l+1}}, \omega_{m_0})]$ to transmit data packets. $L_{T_{l+1}}$ denotes the new location that establishes the link at time point $T_{l+1}$. In the meantime, the LOS path entry in *BLT* is updated with the new link. If the sniff frame results in no response, AP starts to send sniff frames to all potential areas that client could move to.

***2.2 Sniff along potential directions***: If sniffing with the wider beam is not fruitful, *BeamSniff* tries to sniff all the potential directions the client might have moved to. Some approaches attempt to predict next location that client may move to and sends data packets to that direction. In practice, due to the randomness in motion, it is difficult to exactly predict the direction that a client moves to. As shown in Figure

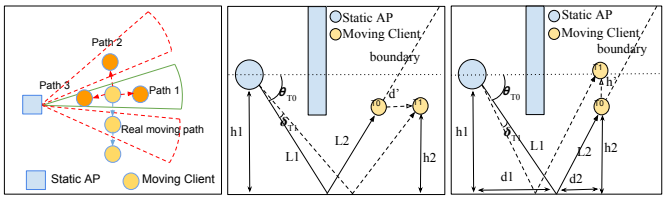


(a) (b) (c)

Fig. 4: A sample scenario where BeamSniff sends sniffing frames to cover all the potential moving directions of the client.

4(a), the client may move along four main directions: left, right, up and down. Potential Path 1 and 3 can still be covered by the current primary sector. The actual Path 2 can be covered by two adjacent beams. In some cases, a client may move out of the scope that two adjoining beams can cover but rarely move out of the scope that three adjacent beams cover on both sides.

Therefore, if sniffing with wider beam fails, AP starts to send sniff frames to adjacent beams $AS^{LS}_{i+1}(L_{T_l}, \omega_{k_0-1})$ and $AS^{LS}_{i-1}(L_{T_l}, \omega_{k_0-1})$. On the other side, if client does not receive any sniff frame with broadening beam width, it will immediately switch to pseudo-omni directional mode. One of the adjacent beam becomes current primary beam sector if client can decode the sniff frame and send response back with that adjacent beam. After setting up the TX sector, client can further refine its beam sector from searching over its previous adjacent beams set:

$$\{[CS^{LS}_{j-x}(L_{T_l}, \omega_{m_0}),\ CS^{LS}_{j+x}(L_{T_l}, \omega_{m_0})] | x \in \{1, 2, 3, ...\}\}$$

Finally new beam sector $[AS^{LS}_{i'}(L_{T_{l+1}}, \omega_{k_0-1}), CS^{LS}_{j'}(L_{T_{l+1}}, \omega_{m_0})]$ becomes new primary sector for data transmission. However, if neither of two adjacent beams of AP could work as TX sector, AP continues to send sniff frames to next adjacent beams $AS^{LS}_{i\pm2}(L_{T_l}, \omega_{k_0-1})$. The same process described above is executed again to find the available beam sector pair. Considering the real case, BeamSniff is set to sniff along at most three adjacent beams on both sides, which means BeamSniff stops sniffing if it still cannot establish a link on sector $AS^{LS}_{i\pm3}(L_{T_l}, \omega_{k_0-1})$.

***2.3 Restart revised BFT***: The last case is that BeamSniff is completely lost and cannot sniff any available transmission path with the above-mentioned procedures. Then BeamSniff enters into the revised BFT training process to search the new possible path. The path entries in *BLT* are also updated during the process. But this case rarely appears in our experiments.

The smart sniffing mechanism only requires at most dozens of sniff frames transmitted. The beam switching and sniff frames transmission take time in the order of $\mu s$, which is negligible compared to the time taken in BFT. Also, we want to mention that when a client stops moving and the link tends to stabilization in a certain time, BeamSniff tries to refine the beam sector with narrower beam width and stronger RSS. But in the mobile circumstance, narrow beam width may frequently lead to the link outage and beam retraining, which makes beam refinement useless.

***3. Prevent link outage for motion under blockage:*** Now we consider a more complicated mobile scenario that includes the humans or objects blockage. As shown in Figure 4(b) and (c), client moves to location $L_{T_0}$ at time $T_0$. Due to blockage of obstacle, AP has to search NLOS path to transit data packets. Assume client just moves to Location $L_{T_0}$ under blockage. The mechanism used for device motion will not work in this scenario. *BeamSniff* has to search a new NLOS path to detour the obstacle. If there is no historical NLOS paths information in *BLT* table to leverage, *BeamSniff* starts to run the revised BFT training procedures to find available NLOS transmission paths and updates the paths in *BLT* table. The new beam sector pair $[AS^{NLS}_{p1,i}(L_{T_0}, \omega_{k_1}),\ CS^{NLS}_{p1,j}(L_{T_0}, \omega_{m_1})]$ with strongest RSS is selected for current communication link. Other NLOS paths with weaker RSS are sorted by strength and also stored in *BLT* table.

Assume link outage happens again when the client moves to new location $L_{T_1}$ at next time point $T_1$. The traditional BFT process is invoked immediately if executing protocol in IEEE 802.11ad. *BeamSniff* leverages the spatial correlation among 60 GHz communication channels to fast sniff next available communication channel with minimum cost. AP intelligently sends minimum sniffing frames to cover all the areas that client may move to. Figure 4(b)(c) shows that the client may move to any position in the left or right area of the boundary line. The solid line in the graph denotes the broken NLOS communication link which was established in location $L_{T_{t0}}$ at previous time point $T_{t0}$. From the graph, the beam sectors $AS^{NLS}_{p1,i+1}(L_{T_0}, \omega_{k1})$ and $AS^{NLS}_{p1,i-1}(L_{T_0}, \omega_{k1})$, which are the adjacent beam sectors of previous location $L_{T_0}$, can cover locations in the left and right area of the boundary. Given the angular difference $\delta_{t1}$ between the current primary sector and its adjacent sector, we can estimate areas that adjacent beams can cover.

Most NLOS links have relatively weak RSS, so sniffing with wider beam leads to low throughput and is not used in the NLOS path searching. Thus, AP sends sniffing frames to these two adjacent sectors first. In the meantime, the client immediately switches to the pseudo-omni directional mode once losing the connectivity. If AP can receive a response from the client in one of the two adjacent beam sectors, AP switches to the new beam sector and instructs the client to further tune its beam pattern. Client searches over the adjacent beam sectors on both sides of previous primary beam sector $CS^{NLS}_{p1,j}(L_{T_0}, \omega_{m_1})$. However, if AP does not receive any feedback from the client, AP continues to send sniffing frames to next two adjacent beam sectors $AS^{NLS}_{p1,i\pm2}(L_{T_0}, \omega_{k1})$ and repeats the same process. In a real scenario, three iterations are enough to find the available communication link.

Normally, AP and client can collaborate to find a new communication link using the first NLOS path information in *BLT* via aforesaid mechanism. But if AP still fails to find a new link, AP queries the *BLT* table and gets the second NLOS path $[AS^{NLS}_{p2,i}(L_{T_0}, \omega_{k_2}),\ CS^{NLS}_{p2,j}(L_{T_0}, \omega_{m_2})]$. AP executes the same mechanism to restart the new link sniffing. If all NLOS paths in the *BLT* table are utilized and still cannot search one new link. AP and client have to execute the modified BFT procedures again to find the new link.

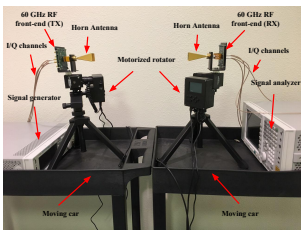


Fig. 5: 60 GHz system platform

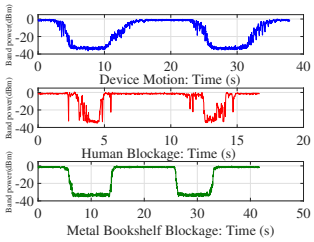


Fig. 6: RSS variation for link failure due to device motion and blockage.

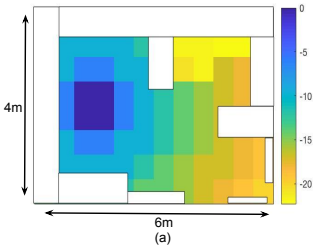


Fig. 7: (a) Variance of received signal strength in the office. (b) Path loss for diverse degrees of horn antenna.

## IV. BeamSniff Implementation and Evaluation

### A. System implementation

***1) Hardware system***: Currently, there are some 60 GHz chipsets and antennas in the market, but no commercial off-the-shelf 60 GHz communication system could be adopted to implement and validate our ideas. Therefore, we build a customized end-to-end 60 GHz communication system to validate our protocol design. Figure 5 illustrates the key components of the system. At the transmitter side, a Keysight EXG N5172B signal generator is used to provide a 10 MHz baseband signal. The baseband signal is fed to a VubIQ 60 GHz transmitter, which up-convert the frequency to 60GHz. The modulated signal is fed to a horn antenna via a waveguide module. At the receiver side, the signal is received by a horn antenna and fed to VubIQ 60 GHz down-converter. The baseband signal is then fed to a spectrum analyzer (Keysight EXA N9010A) to obtain the real-time measurement of the channel's RSS by calculating the power spectral density distribution.

Due to the hardware restriction, we cannot electronically adjust the beam width and fast steer the beam direction in nanoseconds. We use a series of horn antennas with different degree and gains to emulate diverse beam widths. In order to emulate the electronic phased-array based beam steering, we deploy programmable motorized rotators at both transmitter and receiver sides. Beam sweeping and switching are operated mechanically, which emulates the electronic operations in a practical implementation. Furthermore, mobility is emulated by employing moving carts.

***2) Software system***: Due to the hardware constraints, we cannot implement all our protocols and algorithms in the system. Thus we implement a classical ray-tracing [10] based millimeter wave simulator in MATLAB. The LOS/NLOS propagation, path-loss and reflection effects are realized in the simulator and validated against the statistical channel model for IEEE 802.11ad. We implement the protocols and algorithms of *BeamSniff* in this simulator to extensively compare its performance with existing protocols proposed in IEEE 802.11ad and MOCA. In the meantime, we generate the mobility traces of client using random waypoint mobility model. We import the experimental parameters obtained from our measurements and emulated mobility traces to the simulator for validating our system.

***3) Experiment environments:*** We conduct experiments to measure the response of 60 GHz channel variation in one typical $6 \times 4\ m^2$ lab room as depicted in Figure 8(a) that encompasses all potential factors which we want to explore their influence on 60 GHz channel. Typical office objects such as wooden desks, $55''$ LED TV, metal bookshelf, whiteboard, etc. are placed in the room. Some objects in the room could serve as potential reflecting mediums while some of the others could act as obstacles to block the signal. Therefore, signal propagation, attenuation and reflection effect can be obtained in this room.

### B. System evaluation

By using the *BeamSniff* system, we perform over-the-air measurements and conduct many well-designed experiments to evaluate our system.

***1) Device motion:*** We investigate the impact of device motion based on the above experiment environment. With a settled location of the AP, the client is moving up and down along the direction perpendicular to the LOS with the AP. In the meantime, we guarantee that there is no other object blockage between the AP and the client. One snapshot of RSS data variation is given in Figure 6. We can observe that once the client moves out of the area that the current beam sector can cover, the RSS values drop below a cut-off threshold. When the client moves back to the covered area, the RSS recoveries to a normal level. This confirms that device movement can break a link due to the misalignment of the formerly established beam sector pair between the AP and the client.

***2) Obstacle blockage:*** In addition to device movement, we explore human and object blockages in the same experiment setting. First, we fix the location of both the AP and the client and let humans walk randomly in the room which occasionally tears the link down. Figure 6 also exhibits a snippet of RSS data variation in case of humans blockage. The RSS falls off with large fluctuation. The random movement of arms and other body parts may be the reason for drastic signal fluctuation. This is also the reason why we use the second order statistics of RSS values in *Algorithm 1* to distinguish the cause of RSS attenuation and achieve high accuracy. The third sub-graph in Figure 6 presents the scenario when the client moves to the shadow of a metal bookshelf. The tall metal bookshelf blocks the LOS path of signal transmission. In addition to the human and metal bookshelf blockage, we can see many other obstacles that can also obstruct the 60 GHz link, such as water dispenser and desktop computer. The ubiquitous impediments leading to the link outage are becoming the reason for hindering its widespread deployment in the real world.

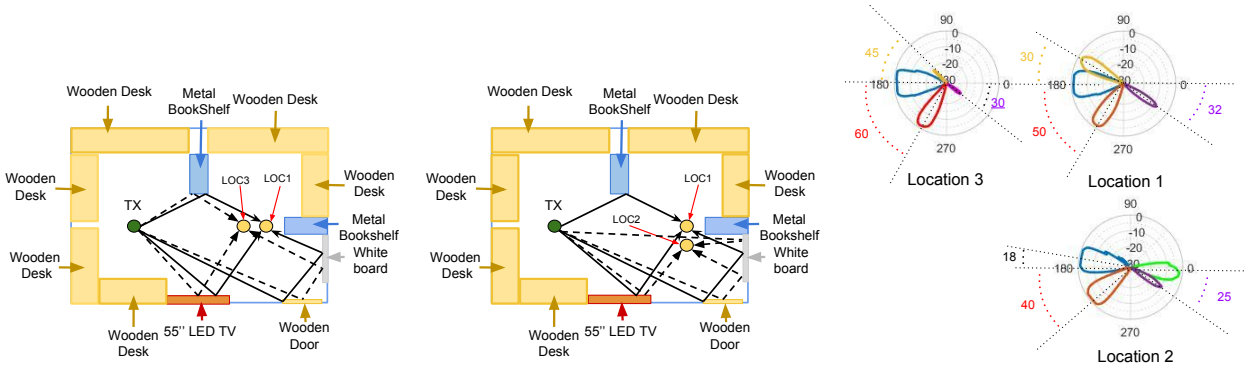


Fig. 8: Spatial correlation of received signal for 60 GHz indoor communication: (a) Transmission paths at LOC 1 and 3. (b) Transmission paths at LOC 1 and 2. (c) Real beam patterns at LOC 1, 2 and 3.

***3) Beam patterns construction for channels:*** We conduct a great number of experiments to investigate the characteristics of indoor 60GHz channels. We place the AP in the left side of the room. The client is arranged at varying locations at a granularity of $0.5 \times 0.5\ m^2$. For every location of the client, we measure the real beam patterns from both sides of the AP and client. Mechanical beam steering is used to emulate real electronic phased-array based beam steering. In order to construct both LOS and NLOS transmission paths, first, we set the AP beam direction to $0°$ and rotate the beam direction of the client by one degree at a time from $0°$ to $360°$. We repeat the procedures to enumerate all possible beam direction pairs. For each direction pair, we collect the RSS data for at least one minute. We write scripts to automatically and precisely adjust the beam direction via controlling motorized rotator. We run the experiments for hundreds of hours and ultimately produce the actual beam patterns for every location of the client, which is shown as in Figure 8(c). After thoroughly analyzing the experimental data, we have some meaningful observations. We clarify the following questions via illustrating the observations of the spatial correlation of indoor 60GHz channels.

***4) Is BeamSniff applicable ?***

BeamSniff tries to fast sniff the new available LOS/NLOS transmission link to repair the broken link. Then we come up with a crucial question: could we discover such LOS/NLOS paths in most positions of indoor environments? For object blockage, a new NLOS path could be used to detour the obstacle via various indoor reflectors. Considering the same room layout as Figure 8(a)(b), we plot the variance of received signal strength in the office. The AP equipped with a $20°$ horn antenna is located in the left side of the room where exposes the strongest signal strength as a mazarine spot in the Figure 7(a). The signal strength is decreasing along with the increment of communication distance. Higher degree antenna implies the broader beam width and more path loss, which is manifested in Figure 7(b). Even though the right top area is under the shadow of the metal bookshelf, the signal can still reach to this area via NLOS paths.

Based on our measurements, the signal from the AP can cover all the areas in most indoor environments via LOS and NLOS paths. Furthermore, the available transmission paths are changing dynamically with the motion of the client. Figure 8(a)(b) displays the transmission paths from three adjoining locations. As shown in the figure, if the client moves from Location 1 to Location 2, the total number of LOS and NLOS paths does not change. But one NLOS path disappears and another new NLOS path appears. The same case is also shown when the client continues to move from Location 2 to Location 3. But we find that in most spots of the indoor environments, there is always at least one NLOS or LOS path available to use for data transmission. Such good feature also demonstrates the *applicability* of our *BeamSniff* system.

***5) Is BeamSniff scalable ?***

***Size and update frequency of BLT***: *BeamSniff* manipulates the BLT table to fast infer a new transmission path. Actually, the BLT table only maintains the available links' information of the latest position. In most of the indoor environments, for each location pair of the AP and the client, there are usually at most four to five LOS and NLOS transmission paths, which is also manifested in Figure 8(c). Whiteboard, wooden door, LED TV screen, metallic surface and other objects could be the potential signal reflector, and the reflection effects also differ from each other. According to the experiment results, the LED TV screen is a relatively better signal reflector. Furthermore, we find that 60 GHz signal could commonly be reflected at most three times. After multiple reflections, most of the RSS decreases below -78 dBm, which can even not support the lowest bit rate (27.5 Mbps) transmission for control frame. The regularly total four or five LOS and NLOS paths in most time results in the same entry size of the BLT table, which is a small path set to be utilized for link inference. The BLT table is utilized to infer the new communication link once the current link is broken. The BLT is updated only after re-establishing the link. The update frequency is strongly correlated with the frequency that link meets outage.

***Beam sniffing cost***: From Figure 8, we can observe that the directions of the LOS and NLOS paths are altered once the client moves. That means the previously established beam sector pairs become invalid and the AP and client have to explore new transmission paths. Fortunately, we find that the beam patterns in three locations reveal some spatial correlation. Although some beams lobes disappear and some others appear with client's motion, we still can deduce that the beam patterns seem to be similar.

TABLE II: Correlation among indoor 60 GHz links

| No. of adjacent beam sweeps used | One | Two | Three |
|---|---|---|---|
| Probability of success | 72.86% | 84.36% | 90.38% |

Precise analysis of the angle of arrivals (AoA) demonstrates that most beam sectors in the previous location are adjacent to the beam sectors of current location no matter whether it is a LOS or NLOS path. Table II summarizes the statistics after analyzing the measurements. We find that $72.86\%$ of all beam sectors can be hunted within one adjacent beam sector of the neighbor locations. The accuracy boosts to $90.38\%$ when searching within three adjacent beam sectors at neighbor locations. From this observation of the spatial correlations, we can predict possible beam directions of a client in current location utilizing the channel information of anterior adjacent location. *BeamSniff* utilizes the spatial correlations of beam patterns between the adjoining locations to deduce the direction of a new link. *BeamSniff* starts to send sniffing frames to the adjacent beam sectors of the path entries in the BLT table. Accordingly, in most situations, *BeamSniff* just needs to send tens of sniffing frames to explore a new link along these directions. The time cost can be controlled within microseconds and it is negligible compared with the exhaustive search in BFT, which also demonstrates the *scalability* of our beam sniffing mechanism.

### C. Performance evaluation

We compare the overhead and performance improvement of *BeamSniff* with IEEE 802.11ad and MOCA [6]. IEEE 802.11ad cannot defeat the mobility and blockage problems efficiently. IEEE 801.11ad possesses a greater possibility of frequently entering into BFT exhaustive search procedure when a client is continuously moving and blocked by obstacles. MOCA does lessen the search space of sector pairs to some extent once a link is broken down. Nonetheless, MOCA still does not work well with client mobility and blockage.

***1) Mobile client in free space:*** Due to the directional characteristic of beams, the movement of the client may lead to a misalignment of the beam sector pair. Before executing BFT procedures, MOCA first transmits sounding frames with a wider beam. The broader beam does overcome the misalignment but sacrifice the transmission rate. In case this procedure fails, MOCA proceeds to send sounding frames via fail-over sectors which are obtained by last BFT procedures. Nevertheless, the mechanism of MOCA is deficient with a mobile client. The advantage of broadening beam may be transient and vanish instantly if the client suddenly moves outside of the area that the wider beam cannot cover. Furthermore, the fail-over paths obtained in last BFT procedures may become invalid if the client moves to a fresh area. Then, MOCA has to execute the BFT procedure again to hunt a new link.

*BeamSniff* intelligently sniffs a new communication link based on the temporal and spatial correlations among indoor 60GHz channels. *BeamSniff* barely needs to execute BFT to discover a new communication link. As client increases its moving speed, the BFT may frequently be invoked in MOCA and IEEE 802.11ad while *BeamSniff* can still sustain much less time cost to establish a new connection.

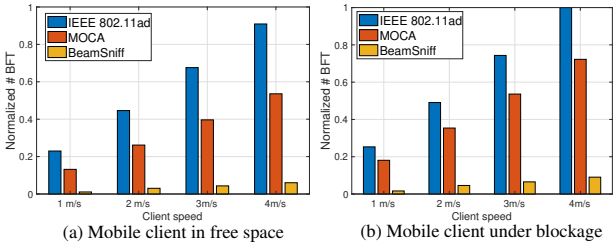

(a) Mobile client in free space (b) Mobile client under blockage

Fig. 9: Number of BFT invocations

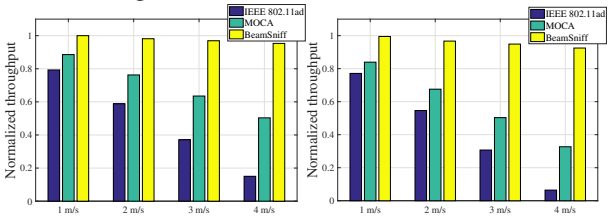

(a) Mobile client in free space (b) Mobile client under blockage

Fig. 10: Throughput obtained by the mobile client

We emulate this scenario with random waypoint mobility model in our simulator. Random waypoint model is one of the most popular mobility models for the movement of mobile users. In this model, a client is moving around in a $10 \times 10m^2$ room. AP is placed in the position of $(5, 5)$, and there is no obstacle in this space. In this experiment setting, we expose the numbers that different protocols enter into BFT procedure with device motion in Figure 9(a). IEEE 802.11ad frequently executes BFT which provokes higher beam searching overhead. MOCA reduces the number to some extent while *BeamSniff* can considerably reduce the probability of invoking BFT. With the increase of movement speed, IEEE 802.11ad and MOCA will more frequently enter into BFT procedure while *BeamSniff* still preserves lower overhead. *BeamSniff* reduces the beam search overhead by $8.89\times$ in average compared with MOCA. Compared with IEEE 802.11ad, the throughput gain increases from $1.13\times$ to $6.34\times$ with client speed changing from 1m/s to 4m/s, which is exhibited in Figure 10(a). *BeamSniff* can obtain more performance gain with increasing client speed.

***2) Mobile client under blockage:*** Now we study a more complex scenario where client moves to the area where obstacles block the signal, and moreover, the client continuously moves under blockage. IEEE 802.11ad will be completely lost in this scenario. For MOCA, a wider beam width cannot surmount the blockage problem, and the fail-sectors from the previous position cannot be utilized for the current position. Consequently, it is challenging for MOCA to find new fail-over sectors while *BeamSniff* wisely sniffs the NLOS fail-over paths via investigating 60 GHz channels' correlation. Sniffing procedure is dynamically changing and adjusted based on real-time movement and blockage of a client. *BeamSniff* has a larger opportunity to promptly discover a new link compared with IEEE 802.11ad and MOCA.

The scenario is emulated with several changes of the previous experiment setting. We place several metal bookshelves that may block the communication links of 60 GHz in the room. A client is moving around inside the room

in accordance with the random waypoint mobility model. Figure 9(b) presents the normalized number of BFT procedures required with mobile client under blockage. IEEE 802.11ad and MOCA perform worse with blockage scenario compared to client motion in free space. BeamSniff still can lessen beam search overhead by $11.06\times$ compared to IEEE 802.11ad with client speed of 4 $m/s$. Figure 10(b) reveals that *BeamSniff* can sustain higher throughput gains of $3.08\times$ and $14.38\times$ than MOCA with client speeds of 3 $m/s$ and 4 $m/s$. IEEE 802.11ad and MOCA exhibit obviously throughput shrinkage compared to Figure 10(a). In conclusion, *BeamSniff* can achieve exceptional performance enhancement both in mobility and blockage scenarios compared with existing protocols about 60 GHz indoor communication.

## V. Related Works

60 GHz networking is widely adopted in various indoor and outdoor environments due to the provision of high multi-Gbps throughput. However, in order to make this into practice, we have to attain the transition from omnidirectional to highly directional transmissions. Due to the stringent requirement of directional transmission, 60 GHz networking faces the challenges [1] of communication link outage under mobility and blockage scenarios. Linear and circular motions of a device are modeled in [11]. The circular motion of the device may break the link more frequently than the linear motion. Humans and objects blockage [12] is another major challenge in 60 GHz communication. The impact of signal attenuation on the presence of a human is measured and characterized in [2].

Existing research works focus on addressing various challenges in 60 GHz networks. A double-link beam tracking scheme [13] is proposed and used for searching transmission and alternative links and detecting human blockage. Environment leaning based beam switching [14] is a feasible technique to resolve link blockage based on the change of environment. E-Mi [15] harnesses 60 GHz radios' sensing capabilities to reconstruct a coarse-grained outline of major reflectors in the environment, which is used for channel prediction. Codebook-based [3], [16], [17] beam switching is a favorite technique to resolve the link-blockage by steering the beam from the blocked path to an alternative path. Instead of single-hop communication, the introduction of relays nodes that enables multi-hop communication can also be a feasible approach to overcome the blockage problem and improve the robustness of 60 GHz links [18], [19]. Pia [20] comprises multiple cooperating APs and leverages the pose information on mobile clients to proactively select the AP and manage multi-link spatial reuse.

## VI. Conclusion

In this paper, we investigate the problem of frequent link re-establishment in 60GHz communication that accompanied by high directional adaptive beamforming antennas. A nominal device motion or obstacle can break the link. Conventional standards use exhaustive spatial search for each link failure. We conduct well-designed experiments to observe the temporal and spatial correlations. Based on the observations, we propose *BeamSniff*, a novel protocol to resolve both mobility and blockage challenges collectively. It uses the observed signal path in recent past to deduce a possible alternative signal path to reinitiate the broken link. *BeamSniff* drastically reduces the beam searching delay while imposing lower overhead, thereby enabling seamless communication in 60 GHz. The quality and robustness of *BeamSniff* is demonstrated on a custom-built 60 GHz system platform along with a ray-tracing simulator. The results manifest a multifold performance improvement concerning throughput and link maintenance overhead.

## References


[1] T. Nitsche, C. Cordeiro, A. B. Flores, E. W. Knightly, E. Perahia, and J. C. Widmer, "Ieee 802.11 ad: directional 60 ghz communication for multi-gigabit-per-second wi-fi," *IEEE Communications Magazine*, vol. 52, no. 12, pp. 132–141, 2014.

[2] S. Collonge, G. Zaharia, and G. E. Zein, "Influence of the human activity on wide-band characteristics of the 60 ghz indoor radio channel," *IEEE Transactions on Wireless Communications*, pp. 2396–2406, 2004.

[3] Z. Yang, P. H. Pathak, Y. Zeng, and P. Mohapatra, "Sensor-assisted codebook-based beamforming for mobility management in 60 ghz wlans," in *MASS'15*, pp. 333–341, IEEE.

[4] T. Nitsche, A. B. Flores, E. W. Knightly, and J. Widmer, "Steering with eyes closed: mm-wave beam steering without in-band measurement," in *INFOCOM'15*, pp. 2416–2424, IEEE.

[5] S. Sur, I. Pefkianakis, X. Zhang, and K.-H. Kim, "Wifi-assisted 60 ghz wireless networks," in *MobiCom'17*, pp. 28–41, ACM.

[6] M. K. Haider and E. W. Knightly, "Mobility resilience and overhead constrained adaptation in directional 60 ghz wlans: protocol design and system implementation," in *MobiHoc'16*, pp. 61–70, ACM.

[7] S. Sur, X. Zhang, P. Ramanathan, and R. Chandra, "Beamspy: enabling robust 60 ghz links under blockage," in *NSDI'16*, pp. 193–206.

[8] S. Sur, V. Venkateswaran, X. Zhang, and P. Ramanathan, "60 ghz indoor networking through flexible beams: A link-level profiling," in *SIGMETRICS'15*, pp. 71–84, ACM.

[9] Z. Xiao, T. He, P. Xia, and X.-G. Xia, "Hierarchical codebook design for beamforming training in millimeter-wave communication," *IEEE Transactions on Wireless Communications*, pp. 3380–3392, 2016.

[10] D. Steinmetzer, J. Classen, and M. Hollick, "mmtrace: modeling millimeter-wave indoor propagation with image-based ray-tracing," in *INFOCOM'16 WKSHPS*, pp. 429–434, IEEE.

[11] M. Park and H. K. Pan, "Effect of device mobility and phased array antennas on 60 ghz wireless networks," in *Proceedings of the 2010 ACM international workshop on mmWave communications: from circuits to networks*, pp. 51–56, ACM, 2010.

[12] Z. Yang, P. H. Pathak, Y. Zeng, X. Liran, and P. Mohapatra, "Monitoring vital signs using millimeter wave.," in *MobiHoc'16*, pp. 211–220.

[13] B. Gao, Z. Xiao, C. Zhang, L. Su, D. Jin, and L. Zeng, "Double-link beam tracking against human blockage and device mobility for 60-ghz wlan," in *WCNC'14*, pp. 323–328, IEEE.

[14] X. An, C.-S. Sum, R. V. Prasad, J. Wang, Z. Lan, J. Wang, R. Hekmat, H. Harada, and I. Niemegeers, "Beam switching support to resolve link-blockage problem in 60 ghz wpans," in *Personal, Indoor and Mobile Radio Communications, 2009 IEEE 20th International Symposium on*, pp. 390–394, IEEE, 2009.

[15] T. Wei, A. Zhou, and X. Zhang, "Facilitating robust 60 ghz network deployment by sensing ambient reflectors.," in *NSDI'17*.

[16] H.-H. Lee and Y.-C. Ko, "Low complexity codebook-based beamforming for mimo-ofdm systems in millimeter-wave wpan," *IEEE Transactions on Wireless Communications*, pp. 3607–3612, 2011.

[17] B. Li, Z. Zhou, W. Zou, X. Sun, and G. Du, "On the efficient beamforming training for 60ghz wireless personal area networks," *IEEE Transactions on Wireless Communications*, pp. 504–515, 2013.

[18] Z. Genc, G. M. Olçer, E. Onur, and I. Niemegeers, "Improving 60 ghz indoor connectivity with relaying," in *ICC' 10*, pp. 1–6, IEEE.

[19] S. Singh, F. Ziliotto, U. Madhow, E. Belding, and M. Rodwell, "Blockage and directivity in 60 ghz wireless personal area networks: From cross-layer model to multihop mac design," *IEEE Journal on Selected Areas in Communications*, vol. 27, no. 8, 2009.

[20] T. Wei and X. Zhang, "Pose information assisted 60 ghz networks: Towards seamless coverage and mobility support," in *MobiCom'17*, pp. 42–55, ACM.